

Translational bypassing without peptidyl-tRNA anticodon scanning of coding gap mRNA

Norma M Wills¹, Michelle O'Connor^{1,2},
Chad C Nelson³, Charles C Rettberg¹,
Wai Mun Huang⁴, Raymond F Gesteland¹
and John F Atkins^{1,2,*}

¹Department of Human Genetics, University of Utah, Salt Lake City, UT, USA, ²BioSciences Institute, University College Cork, Cork, Ireland, ³Mass Spectrometry and Proteomics Core Facility, University of Utah, Salt Lake City, UT, USA and ⁴Department of Pathology, University of Utah, Salt Lake City, UT, USA

Half the ribosomes translating the mRNA for phage T4 gene 60 topoisomerase subunit bypass a 50 nucleotide coding gap between codons 46 and 47. The pairing of codon 46 with its cognate peptidyl-tRNA anticodon dissociates, and following mRNA slippage, peptidyl-tRNA re-pairs to mRNA at a matched triplet 5' adjacent to codon 47, where translation resumes. Here, in studies with gene 60 cassettes, it is shown that the peptidyl-tRNA anticodon does not scan the intervening sequence for potential complementarity. However, certain coding gap mutants allow peptidyl-tRNA to scan sequences in the bypassed segment. A model is proposed in which the coding gap mRNA enters the ribosomal A-site and forms a structure that precludes peptidyl-tRNA scanning of its sequence. Dissipation of this RNA structure, together with the contribution of 16S rRNA anti-Shine–Dalgarno sequence pairing with GAG, facilitates peptidyl-tRNA re-pairing to mRNA.

The EMBO Journal (2008) 27, 2533–2544. doi:10.1038/emboj.2008.170; Published online 4 September 2008

Subject Categories: RNA; proteins

Keywords: mRNA folding; ORF coupling; ribosomal frame-shifting; ribosome; translational bypassing

Introduction

Linear scanning from the 5' end of mRNAs by 40S ribosomal subunits seeking translation start sites is a general hallmark of eukaryotic protein synthesis. Scanning by the smaller eubacterial ribosomal subunit, 30S, is less well known, but in some cases, it may move from a standby site into the final initiation site (Unoson and Wagner, 2007). Also, in some cases following termination, the 30S subunit scans with the potential to find reinitiation codons (Klovins *et al.*, 1997; Wills *et al.*, 1997; Jin *et al.*, 2006). Important exceptions to the universality of linear scanning for eukaryotic translation initiation occur where there is internal ribosome entry, and also where the scanning is nonlinear. The latter, known as

ribosome shunting, has been studied in decoding of some cellular mRNAs from mammals to an alga and especially in several viral mRNAs, including cauliflower mosaic virus and adenoviruses (Hemmings-Mieszczak *et al.*, 2000; Xi *et al.*, 2005; Babinger *et al.*, 2006). Adenovirus shunting may involve rRNA:mRNA interactions in translating ribosomes (Yueh and Schneider, 2000; Chappell *et al.*, 2006). Translating 'whole' ribosomes also exhibit the ability to bypass mRNA segments and resume translation at a downstream site to synthesize one polypeptide from two open reading frames (ORFs), or a polypeptide lacking internal sequence from a single ORF. Such translational bypassing was initially discovered as low-level 'error' bypassing of stop codons, 'stop hopping', in *Escherichia coli* (Weiss *et al.*, 1987; O'Connor *et al.*, 1989). In one of these cases, the 9 nt sequence CUU_UAG_CUA encoded a single amino acid, leucine. The anticodon of peptidyl-tRNA^{Leu} dissociates from pairing with the CUU, the 'take-off' codon, and scans the mRNA as it linearly slips through the ribosome. The anticodon re-pairs to mRNA where it finds complementarity, that is, at the 3' CUA, the 'landing-site' codon. Standard decoding then resumes at the next codon. Short distance stop codon bypassing also occurs at the end of the β -globin mRNA of rabbits (Chittum *et al.*, 1998). Similar bypassing involving peptidyl-tRNA anticodon scanning also occurs where, in place of the slow-to-decode stop codon, there is a codon in which aminoacyl-tRNA is severely limiting ('hungry' codon bypassing) (Kane *et al.*, 1992; Gallant and Lindsley, 1998; Gallant *et al.*, 2003). This bypassing can be over considerable mRNA distances (Gallant and Lindsley, 1998). Bypassing, in general, allows ribosomes to escape a barrier or enter an alternative frame, as it is frame independent. However, the efficiency of these cases of non-programmed bypassing is low and biological utility has not yet been demonstrated. Even with error bypassing, re-pairing to mRNA occurs predominantly at cognate codons, though re-pairing to mRNA at codons that permit only poor Watson–Crick or wobble pairing is detectable at a low level (Herr *et al.*, 2004).

In contrast, the programmed translational bypassing required for decoding phage T4 gene 60 (Huang *et al.*, 1988; Weiss *et al.*, 1990) occurs at a high level. In phage T4, separate genes 39 and 60 correspond to a single gene 39 in phage T2, representing the common ancestral state (Figure 1). In phage T4, an insertion of 1010 nt occurs after gene 39 codon 473 and contains a derivative of a *mob A* homing endonuclease, as well as, an ORF termed gene 60.1 (for review, see Miller *et al.*, 2003). Recent work has shown that *mobA* and 60.1 comprise a single continuous ORF (DA Shub, Personal communication). The 3' 93 nt of this insertion encode the first 31 amino acids of the T4 gene 60 product. A second insertion, 50 nt, is found between codons 46 and 47 of gene 60, the gene product of which is an essential topoisomerase subunit. The 50 nt coding gap contains stop codons in all three frames (Huang *et al.*, 1988). When a cassette containing the gene 60 segment important for bypassing is expressed in *E. coli* cells, half the

*Corresponding author. Department of Human Genetics, University of Utah, Salt Lake City, UT, USA. Tel.: +1 801 585 3434; Fax: +1 801 585 3910; E-mail: john.atkins@genetics.utah.edu

Received: 14 March 2008; accepted: 6 August 2008; published online: 4 September 2008

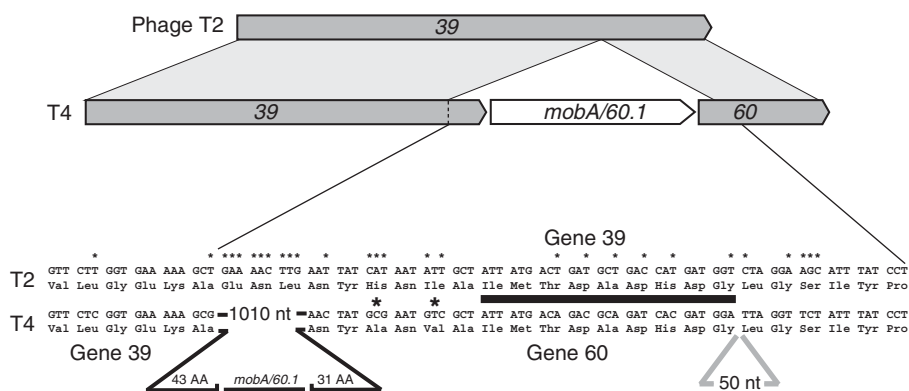


Figure 1 Comparison of phage T2 gene 39 with its phage T4 counterpart. One large insertion of 1010 nt containing *mobA/60.1* in the common ancestral gene 39 arrangement present in T2 produces separate genes, 39 and 60, in phage T4. In phage T2, gene 39 encodes gene 60 function at its distal end as indicated by the darkly shaded boxes. A second insertion of 50 nt occurs between codons 46 and 47 of T4 gene 60. The underlined amino acid sequence is a signature for topoisomerases. Nucleotide differences between the two phages are denoted by * and amino acid differences by *.

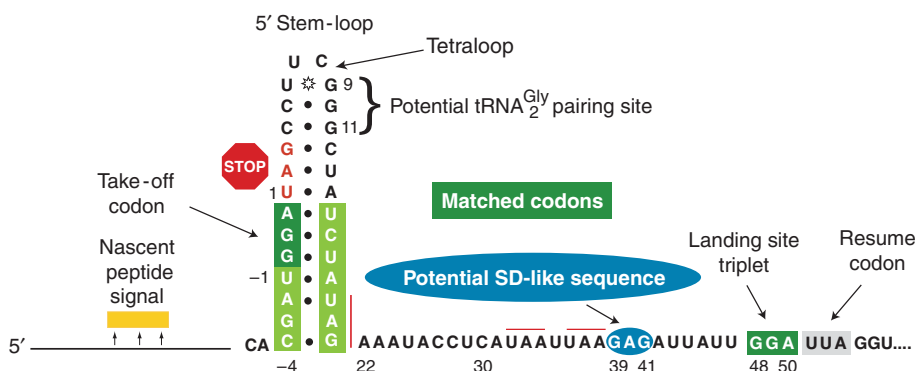


Figure 2 Features important for translational bypassing in decoding T4 gene 60. The nascent peptide signal is indicated by the yellow box; the matched take-off and landing codons, GGA, are shown in white letters in dark green boxes; the UAG stop codon immediately 3' of the take-off site is in red letters next to the stop sign; stop codons within the coding gap are overlined in red; and sequences that may be involved in base pairing in a potential extension of the stem-loop are boxed in light green. A Shine-Dalgarno-like sequence is shown in the blue oval. The translational resume codon is indicated by the gray box.

ribosomes bypass the 50 nt coding gap present in mature mRNA (Herr *et al*, 2000a). This bypassing is programmed in the sense that several mRNA recoding signals are necessary for it to occur (Figure 2) (Weiss *et al*, 1990; Herr *et al*, 2000b). One component is the UAG codon immediately 3' of the take-off codon. This UAG codon is involved in base pairing within a stem-loop structure shown to be important for efficient bypassing (Weiss *et al*, 1990). A potential elongated 5' stem-loop is shown in Figure 2 and the remainder of the coding gap sequence is depicted linearly.

In addition to the stem-loop, another recoding signal is a segment of the nascent peptide encoded 15–30 codons 5' of the take-off site (Weiss *et al*, 1990). While still within the ribosome, this region has a nine-fold effect on bypassing efficiency (Herr *et al*, 2001a). It facilitates codon:anticodon dissociation at the take-off site and continues to exert an effect so that it has an effect in imposing landing site fidelity (Herr *et al*, 2000a, 2000b, 2004).

Expression of a cassette of the gene 60 sequence shows that the anticodon of peptidyl-tRNA₂^{Gly} (Herr *et al*, 1999) detaches from the glycine codon 46, GGA, in all ribosomes translating the mRNA (Herr *et al*, 2000b; Bucklin *et al*, 2005). (Factors that influence ribosomes that do not successfully bypass the gap have been analysed separately (Herr *et al*, 2001b)). Consistent with complete take-off, debilitation of

release factor 1 (RF1), which mediates termination at UAG, does not elevate the level of gene 60 bypassing, though it greatly elevates bypassing with a simple stop hop control (Herr *et al*, 2000b). (Yet overexpression of RF1 does reduce gene 60 bypassing.) After take-off, in half of the ribosomes, the peptidyl-tRNA anticodon re-pairs to mRNA at the next GGA, 48–50 nt 3', so that productive translation resumes at the 3' adjacent codon, the resume codon. GGA is solely decoded by tRNA₂^{Gly}, which also decodes GGG (Murgola and Pagel, 1980). Interestingly, there is a GGG triplet at positions 9–11 within the coding gap.

In a scanning model, the anticodon of peptidyl-tRNA₂^{Gly} would continuously monitor the coding gap sequence as it moves through the ribosome, the same mechanism employed in stop hopping (Herr *et al*, 2001a). If peptidyl-tRNA scanning occurs, landing would be expected at GGG_{9–11} and result in termination at a UAA stop codon, 24 nt 3'. This study was undertaken to elucidate the mechanism for traversing the coding gap.

Results

Fidelity of landing

Mass spectrometry of the product(s) translated from a gene 60 bypass cassette reveals the amino acid encoded by the translation resume codon. As productive peptidyl-tRNA

re-pairing to mRNA occurs at the 5' adjacent triplet, landing site triplets can be directly deduced from product analysis. Where multiple but closely related products are present, the relative peak intensities observed from electrospray mass spectrometric analysis of intact proteins are a reflection of the relative abundance of each of the proteins in the mixture (Herr *et al*, 2004). However, for analysis of a mixture of proteins with completely different sequences, electrospray mass spectrometry will not be quantitative. In the cases presented here, each of the bypass products (as distinct from the non-bypass product) is similar, apart from a small number of residues, such that relative peak intensities are a reasonably good indicator of relative protein abundance. Nevertheless, we have exercised caution in making strict quantitative interpretations based on mass spectrometry data.

The wild-type (WT) gene 60 bypassing cassette, as defined by earlier work, was inserted into modified vector pNTH-2 (Nus Tri-His-2), 3' of sequences encoding the highly soluble NusA protein, a 6 × His tag, and an S-tag epitope (Figure 3A). Affinity-purified protein(s) was subjected to electrospray ionization mass spectrometry (ESI/MS). As the 6 × His tag and S-tag are located N-terminal to the gene 60 take-off site, all bypass and non-bypass products should be evident. Only two products were detected, one due to take-off without successful landing and the other due to landing at GGA₄₈₋₅₀, showing the high fidelity of bypassing (Figure 3B and C). There was no evidence of landing at other triplets within the gap; of particular interest, there was no landing at GGG₉₋₁₁, a potential peptidyl-tRNA^{Gly} pairing site (Figure 3B and C). However, as GGA₄₈₋₅₀ is the only tRNA^{Gly} pairing site in the vicinity of the WT landing site, the inherent potential for landing at nearby locations could not be assessed in the WT context.

To address the potential for landing at sites 5' of the WT position, the take-off and landing site codons were changed to AUU. As the identities of the two WT codons preceding the WT landing codon are also AUU, this results in three tandem AUU codons (compensatory changes were made to retain take-off stem-loop pairing potential as described in Materials and methods). (In this and all subsequent constructs, the 6 × His tag immediately 3' of NusA was removed and 6 × His tags in each of the three reading frames were added 3' to the gene 60 cassette to allow purification of bypass products containing C-terminal tags and to prevent co-purification of the non-bypass product (Figure 4A).) In this construct with four potential AUU landing sites (the above three and one at positions 34–36), only the WT-positioned AUU₄₈₋₅₀ codon was utilized (Figure 4B and C). To further address the propensity for landing in the vicinity of the normal site, the GGA take-off and landing sites were changed to UCC and the landing site was followed by five additional UCC triplets (Figure 5). (UCCs were chosen as the matched take-off and landing site codons as they do not contain A or G (see below) and they substitute well for the WT GGA take-off and landing codon set (see Bucklin *et al*, 2005).) With this construct, all landing occurred at UCC₄₈₋₅₀, the position of landing in WT, and none at the potentially competitive 3' adjacent UCC triplets (Figure 5).

The above experiments show that landing does not occur at matched codons located either immediately 5' or 3' of the normal landing site position when in competition with the

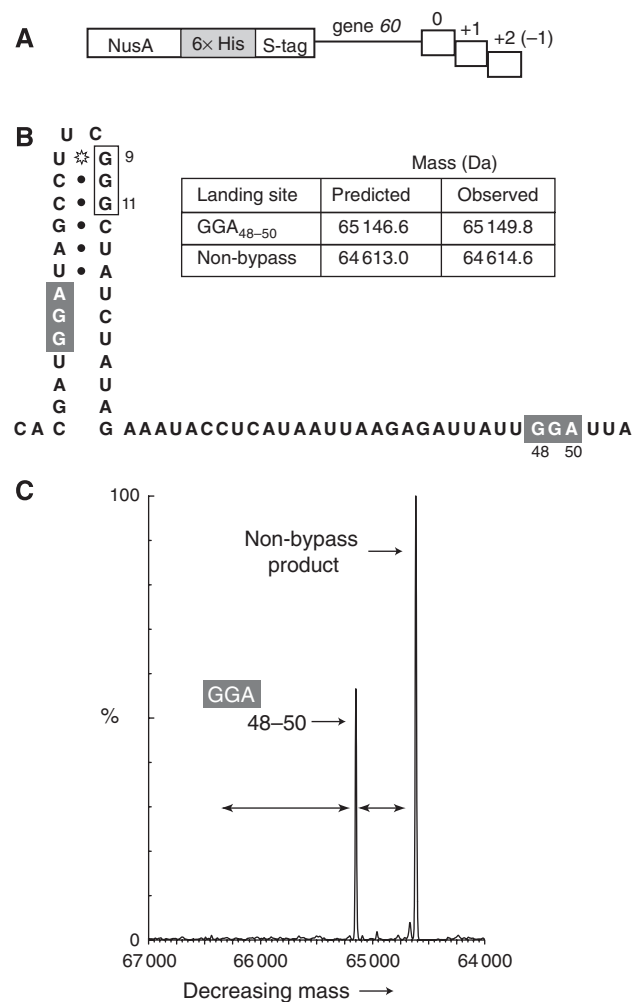


Figure 3 Bypassing with a WT gene 60 cassette. (A) Cartoon of the *E. coli* expression vector for analysing bypassing product(s). Sequences for two affinity tags, 6 × His and S-tag, are located 5' of gene 60 sequences allowing for purification of both productive (bypass) and non-productive (non-bypass) products. (B) Sequence and potential secondary structure of the coding gap region. Matched take-off and landing codons are shaded in grey. The potential lower part of the 5' stem-loop is shown unpaired. The potential peptidyl-tRNA^{Gly} pairing site, GGG₉₋₁₁, is boxed. Predicted and observed masses of products from mass spectrometry analysis are indicated. (C) Neutral mass spectrum of protein products. Mass is shown on the x axis, decreasing from left to right, and abundance is shown on the y axis. The double-headed arrows indicate mass ranges of products predicted from landing elsewhere within the coding gap.

same codon at the WT landing position. To more finely address the potential for landing near the WT position, a construct was designed containing an AAA take-off site and AAA₄₈₋₅₀ landing site followed by AAA₅₁₋₅₃. This construct allows for landing in different reading frames at overlapping AAA codons spaced one nucleotide apart. (This approach was not suitable for evaluating a longer stretch of overlapping AAA codons as runs of >8 Ts in the DNA template are susceptible to transcriptional slippage in *E. coli* (Larsen *et al*, 2000).) The most abundant product results from landing at AAA₄₈₋₅₀, the WT position, although a significant amount of product results from landing at AAA₅₀₋₅₂, AAA₄₉₋₅₁ or AAA₅₁₋₅₃ (Supplementary Figure S1). This most likely reflects the difference in pairing potential of peptidyl-tRNA^{Lys} with AAA compared with peptidyl-tRNA^{Gly} with GGA, in the gene 60

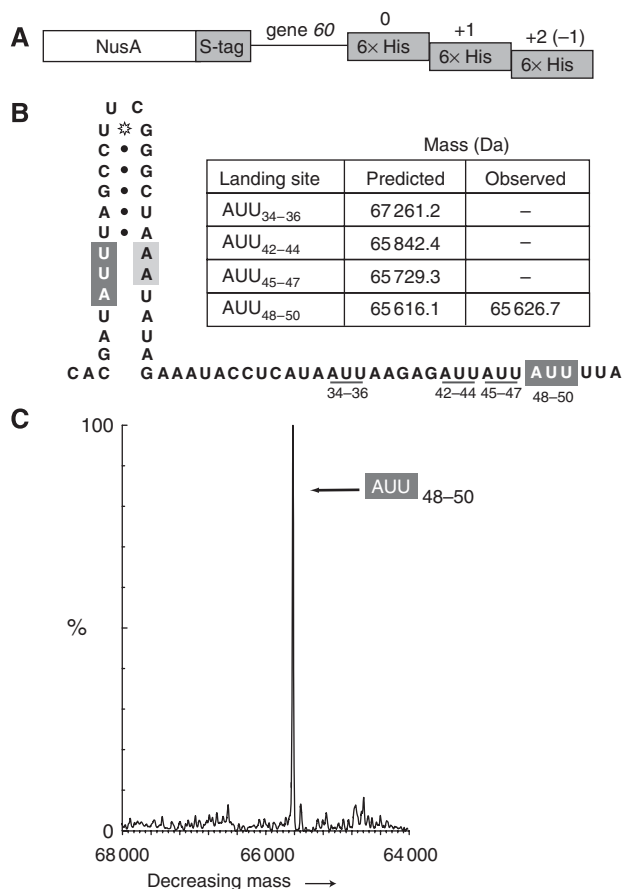


Figure 4 Landing in construct with matched AUU take-off and landing sites. (A) Cartoon of the *E. coli* expression vector. The S-tag and three 6 × His tags (one in each reading frame) are shaded. (B) Sequence and potential secondary structure of the coding gap region. The AUU take-off and WT-positioned landing sites are shaded in dark grey, compensatory base changes are shown in light grey, and three potential WT AUU landing sites are underlined. Predicted and observed masses of potential bypass products are indicated. (C) Neutral mass spectrum of the bypass product(s). Mass is shown on the x axis, decreasing from left to right, and abundance is shown on the y axis.

context (Bucklin *et al*, 2005). No landing is evident at two other potential productive landing sites, AAA₂₂₋₂₄ and AAG₃₇₋₃₉, both decoded by the single tRNA^{Lys} species. The conclusion from these experiments is that peptidyl-tRNA sampling initiates near nucleotide position 48 of the coding gap.

Shine-Dalgarno sequence effect on bypassing

Prior work on *E. coli* RF2 and *dnaX* programmed frame-shifting has shown that translating ribosomes sense Shine-Dalgarno (SD) signals within coding sequences (Weiss *et al*, 1987; Larsen *et al*, 1994) and there is evidence that bypassing 70S ribosomes behave similarly (Herr *et al*, 2004). A minimal SD-like sequence, GAG, is located 6 nt 5' of the WT landing site, a distance corresponding to the optimal distance of a SD sequence involved in initiation (Chen *et al*, 1994; Jin *et al*, 2006). This distance is quite distinct from the different distances used to promote forward or backward realignment in +1 or -1 frameshifting, respectively (Larsen *et al*, 1994).

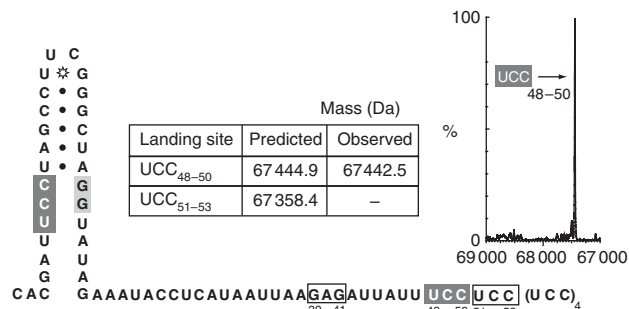


Figure 5 Bypassing with take-off codon, UCC, and multiple, matched landing triplets. Sequence and potential secondary structure of the coding gap region. Matched UCC take-off and WT landing position codons, dark grey. UCC₄₈₋₅₀ is followed by five additional UCC triplets. Nucleotide substitutions to maintain potential base pairing in the 5' stem-loop are shown in light grey. Predicted and observed masses of bypass products are indicated. Neutral mass spectrum of bypass product(s) is shown on the right. Mass is shown on the x axis, decreasing from left to right, and abundance is shown on the y axis.

To assess the effect of the SD-like sequence in the WT gene 60 context, GAG₃₉₋₄₁ was mutated to either CAC₃₉₋₄₁ or GGAGG₃₈₋₄₂, to weaken or strengthen an SD:anti-SD interaction, respectively. For these constructs, the WT or mutant gene 60 cassettes were cloned into a GST-*lacZ* (GLZ) vector such that expression of *lacZ* was dependent on productive bypassing, monitored by β-galactosidase activity. Weakening the potential SD:anti-SD interaction with CAC₃₉₋₄₁ resulted in an ~50% decrease in bypass efficiency relative to WT (Table I). Strengthening the potential SD:anti-SD interaction with GGAGG₃₈₋₄₂ also decreased bypassing to ~40% of WT (Table I). Bypassing efficiencies determined by pulse-chase experiments (Supplementary Figure S2) were consistent with those determined by β-galactosidase activities. These results suggest a role for the GAG₃₉₋₄₁ in gene 60 bypassing, but no conclusion is drawn about the optimal strength of the SD:anti-SD interaction due to possible competing effects on relevant RNA structure (see Discussion).

Specialized ribosomes

To test for a direct interaction between the gene 60 SD-like GAG₃₉₋₄₁ sequence in the coding gap and 16S rRNA, a system utilizing specialized ribosomes was employed. A plasmid carrying the *rnmB* operon was mutated such that the 3' sequence of WT 16S rRNA, 3'-AUUCCUCC-5', was changed to 3'-AUUGGAGG-5', thereby disrupting any potential WT SD:anti-SD interactions. A second plasmid containing the gene 60 bypass cassette in the *lacZ* reporter vector was introduced into strains containing the mutant *rnmB* plasmid. The reporter gene had its initiator SD sequence mutated to CCUCC to facilitate initiation in the presence of the mutant 16S rRNA. Finally, mutations of the SD-like sequence in the coding gap of gene 60 were introduced substituting GAG₃₉₋₄₁ with CUC₃₉₋₄₁ or CCUCC₃₈₋₄₂, both complementary to the mutant anti-SD sequence. In the construct where the coding gap sequence contained CUC₃₉₋₄₁, the bypass efficiency was 67% greater than that of the WT GAG sequence (Table I). Changing the potential SD-like sequence to CCUCC₃₈₋₄₂ resulted in a 36% increase in bypassing over WT GAG (Table I). The control constructs gave complementary results. In the

Table I SD-like nature of WT GAG_{39–41}

WT anti-SD ^{3'} AU <u>UCCUCC</u> ^{5'}		β-gal. units	% GAG _{39–41} bypassing
Initiating SD	Internal SD		
GGAGG	GAG _{39–41}	1066.3 ± 25.3	100.0 ± 2.3
GGAGG	CAC _{39–41}	510.6 ± 19.9	47.9 ± 3.9
GGAGG	GGAGG _{38–42}	422.1 ± 16.5	39.6 ± 3.9
Mutant anti-SD ^{3'} AUUGGAGG ^{5'}		β-gal. units	% GAG _{39–41} bypassing
Initiating SD	Internal SD		
CCUCC	GAG _{39–41}	300.5 ± 9.1	100.0 ± 3.1
CCUCC	CUC _{39–41}	501.8 ± 18.5	167.0 ± 3.7
CCUCC	CCUCC _{38–42}	408.7 ± 24.5	136.0 ± 6.0
GGAGG	GAG _{39–41}	10.1 ± 0.3	100.0 ± 3.1
GGAGG	CUC _{39–41}	14.9 ± 0.4	147.5 ± 2.5
GGAGG	CCUCC _{38–42}	12.1 ± 0.2	120.0 ± 1.7

Potential SD: anti-SD interactions are indicated by shaded sequences.

presence of the mutant 16S rRNA, where initiation utilizing a WT SD sequence, GGAGG, would be much less efficient, the WT internal GAG resulted in very low activity (defined as 100%). Changing the internal SD-like sequence to CUC or CCUCC resulted in increased bypassing to 147 and 120%, respectively (Table I). These results demonstrate that the GAG_{39–41} sequence in the coding gap exerts an effect as an SD sequence by interacting with the 3' end of 16S rRNA.

The experiments described above show that the SD-like sequence in the coding gap, GAG_{39–41}, affects the efficiency of bypassing. The SD-like sequence may also exert an effect by influencing the position of peptidyl-tRNA landing. This was initially tested using a construct containing the UCC take-off site and multiple, tandem UCC landing codons, where GAG_{39–41} was changed to CAC. In this construct, the predominant product resulted from landing at the WT position, 48–50 (UCC), but landing was also detected at UCC_{51–53} (Supplementary Figure S3) in contrast to the situation where the SD-like sequence is present (Figure 5). This suggests a minor role for the SD-like sequence in landing site selection with a related effect on bypassing efficiency.

Introduction of additional SD-like sequences into the coding gap

To further assess the role of the GAG sequence in influencing landing site selection, a series of constructs was made in which a particular GAG sequence within the coding gap could potentially serve either as an SD or a landing site, or both. The parent construct for this series contained GAG at the take-off and landing sites and the WT SD-like GAG_{39–41} sequence 6 nt 5' of the WT landing position. In addition, A₃₇ was changed to C to eliminate a –1 frame stop codon that is pertinent to derivative constructs described below. Landing was observed only at GAG_{48–50} (Supplementary Figure S4), the position of landing in WT, indicating that the SD-like GAG_{39–41} was not being scanned by the peptidyl-tRNA. A GAG_{30–32} sequence was then introduced 6 nt 5' of the WT SD-like GAG_{39–41}. If the introduced GAG_{30–32} can function as an SD to promote scanning of the peptidyl-tRNA, then landing would be expected at the WT SD-like GAG_{39–41}. Landing was observed at GAG_{39–41}, GAG_{48–50} and unexpectedly at GAG_{30–32} (Figure 6A). Although the landings at GAG_{39–41} and GAG_{48–50} are easily interpreted by the presence of preceding SD-like

sequences, the landing at GAG_{30–32} is less readily explained as it is preceded by only a very weak SD-like sequence, GAA_{21–23}, 6 nt 5'. However, an alternative explanation is that the base substitutions in this construct disrupt mRNA structure resulting in landing at sites lacking a suitable SD-like sequence 5'. Such mRNA structure disruption could lead to premature initiation of scanning by the anticodon of peptidyl-tRNA.

The last construct of the series with GAG in place of GGA at the WT take-off and landing sites contained internal GAGs at positions 21–23, 30–32 and 39–41. Landing occurred predominantly at GAG_{30–32}, but trace amounts were evident at GAG_{39–41} and at GAG_{48–50}, the position of landing in WT (Figure 6B). Given the modest contribution of SD-like GAGs to landing at potential sites 6 nt 3' (see above), the high proportion of the landing at GAG_{30–32} in this case, also likely reflects, in part, the consequences of internal mRNA structure disruption. The simplest explanation for the SD effect is that the entire coding gap, based on the 60% tested, is scanned by the anti-SD sequence at the 3' end of 16S rRNA of bypassing ribosomes and that interaction with SD-like sequences in the mRNA facilitates the initiation of scanning by the anticodon of peptidyl-tRNA.

Destabilization of the upper portion of the 5' stem-loop

The upper portion of the 5' stem-loop, capped by a tetraloop (Figure 2) is involved in efficient bypassing (Weiss *et al*, 1990; Herr *et al*, 2000a). However, landing site fidelity was not explored in the earlier studies. Two mutants were constructed to destabilize this region and tested for effects on landing fidelity. To detect any landing 5' of, and in the same frame as, the WT landing site GGA_{48–50}, an A₃₇ to C substitution was made to change a UAA_{36–38} stop codon to UCA. In one Upper Stem mutant, US-1, U₆ was changed to G disrupting the UUCG tetraloop. Landing in this construct occurred at the WT landing site GGA_{48–50}, as well as, a small amount at GGG_{9–11} (Supplementary Figure S5). A second mutant, US-2, with CC_{4,5} to GG substitutions, predicted to disrupt the top of the stem, showed products of landing at alternative sites, GGG_{9–11} and a very small amount at GGG_{3–5}, as well as, the WT landing product (Figure 7A). (The landing at GGG_{3–5} is an example of hopping onto a stop codon where the landing site comprises part of the stop codon (O'Connor *et al*, 1989; Herr *et al*, 2001a).) A control construct was made to test whether the A₃₇ to C substitution alone affected landing and only the product from landing at GGA_{48–50} was observed (data not shown). These data show that disruptions of the upper region of the 5' stem-loop structure allow peptidyl-tRNA₂^{Gly} to productively pair with GGG_{9–11} and mutant GGG_{3–5}. This does not occur in WT bypassing where GGG_{9–11} is normally 'hidden'. The diminished efficiency of bypassing with disruptive mutants in the upper part of the stem-loop (Weiss *et al*, 1990; Herr *et al*, 2000a) is consistent with these results as landing at GGG_{9–11} is non-productive in the WT context due to an in-frame UAA stop 8 codons 3'.

Extent of the lower portion of the 5' stem-loop

Three constructs were designed to address the importance of the potential lower part of the 5' stem-loop (Figure 2): LS-1 (Lower Stem) where base pairing was precluded in the first four positions in the proposed stem (Supplementary

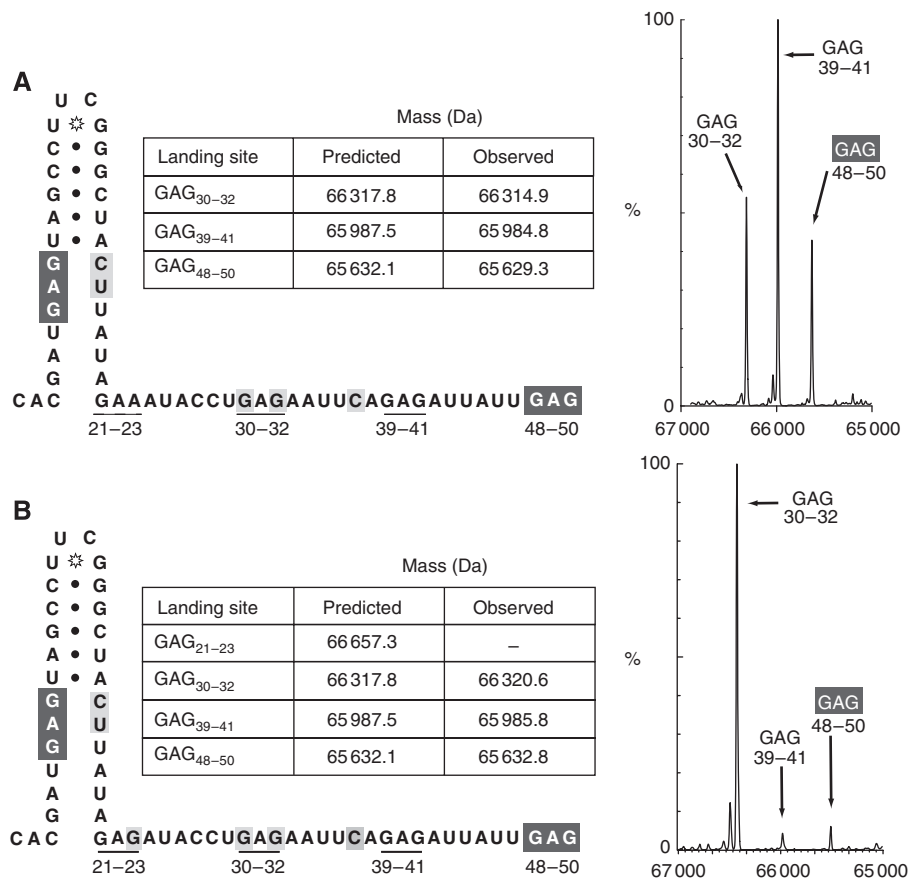


Figure 6 Introduction of potential SD-like GAG sequences into coding gap. **(A)** Construct with GAG introduced at positions 30–32, 6 nt 5' of WT SD-like GAG_{39–41}. The take-off codon and WT-positioned landing site were changed to GAG (dark grey). Potential base pairing of the take-off site was maintained by making compensatory base changes (shown in light grey). A₃₇ was changed to C, light grey, to eliminate a UAA stop codon in-frame with GAG_{30–32}. Potential GAG landing sites 5' of the WT-positioned GAG are underlined. GAA_{21–23}, a weak SD-like sequence is underlined with dashes. Predicted and observed masses of bypass products are indicated. The neutral mass spectrum is shown on the right. Mass is shown on the x axis, decreasing from left to right, and abundance is shown on the y axis. **(B)** Same as in (A) except that A₂₃ was changed to G, shaded in light grey, to create an additional GAG sequence 6 nt 5' of GAG_{30–32}.

Figure S6); LS-2 where potential base pairing of the GGA take-off site was, in addition, disrupted (Figure 7B) and LS-3 where stronger base-pairing potential exists (Figure 7C). With the weakened 5' stem-loop mutants, LS-1 and LS-2, two landing sites were observed, GGA_{48–50} and GGG_{9–11} (Supplementary Figure S6 and Figure 7B). Landing at GGG_{9–11} in the stem-loop mutants, but not in WT, indicates that the stem-loop is somehow involved in masking this potential landing site. With both mutants, bypassing efficiency is substantially reduced (manuscript in preparation). In the strengthened 5' stem-loop construct LS-3, there is no landing at GGG_{9–11}, and the predominant product is due to landing at the WT landing site, GGA_{48–50} (Figure 7C). The efficiency of bypassing with the strengthened stem-loop is slightly greater than WT (manuscript in preparation).

When does the 5' stem-loop exert its effect?

An important difference between an earlier proposed stem-loop and the extended stem-loop tested above is that the GGA take-off codon is base-paired in the extended structure. Therefore, the 5' stem-loop must exert its effect either before or after decoding of the take-off GGA, and the latter was experimentally addressed. If the stem-loop forms within the ribosome after take-off, then mRNA must be pulled backwards

from the P-site to allow base pairing of nt 5' of the take-off GGA, thereby positioning the 3 nt immediately 5' of the stem in the P-site. This was tested by placing a potential landing site 5' adjacent to the base of the stem. The take-off codon was changed to UCC and an A → C substitution 5 nt 5' of the take-off site created a UCC codon at positions –7 to –5 in the –1 reading frame (Figure 8A). (The WT landing site was retained to preclude efficient forward bypassing as potential backwards bypassing was expected to be, at most, a low-level event.) Using LC/MS/MS (with Fourier transform-ion cyclotron resonance (FT-ICR)), a chymotryptic trans-frame peptide was identified that showed backwards bypassing to UCC_{–7 to –5} (Figure 8B and Supplementary Figures S7–S10). This peptide contains 13 amino acids from the 0 frame and 3 amino acids from the –1 frame. Its identity and sequence are confirmed by several criteria: (a) the doubly charged molecular ion in the primary mass spectrum (i.e. acquired in the FT-ICR portion of the LTQ-FT instrument; error of 4 p.p.m.) (Supplementary Figure S10), (b) high sequence coverage observed for both 'b' and 'y' series fragment ions in the MS/MS data of the doubly charged ion (i.e. acquired in the linear ion-trap portion of the LTQ-FT mass spectrometer) (Figure 8B and Supplementary Figure S8) and (c) a high overall score for the peptide sequence from a Mascot™

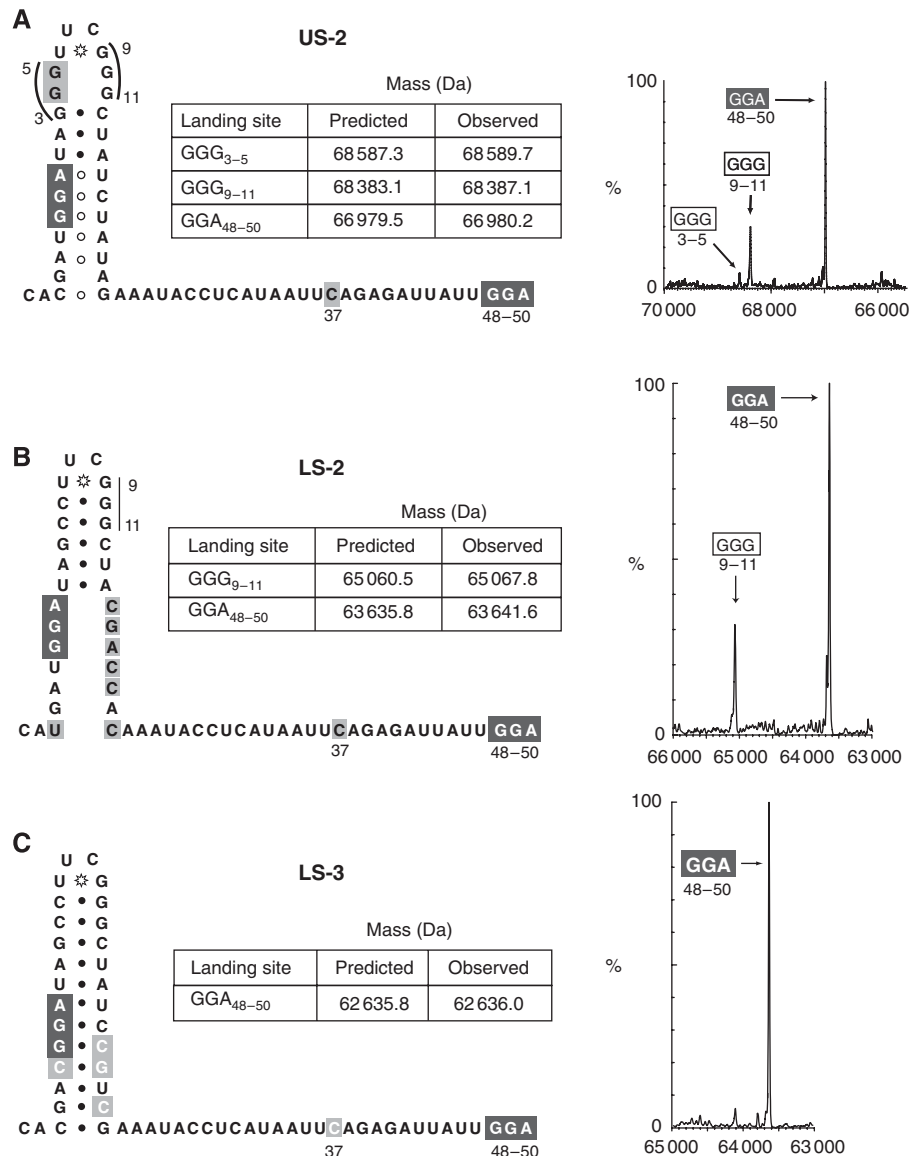


Figure 7 Bypassing with mutants of the 5' stem-loop. (A) Substitution of CC_{4,5} with GG, shown in light grey, disrupts base pairing in the upper part of the stem-loop. A₃₇ was changed to C, light grey, to eliminate a UAA stop codon in-frame with GGA₄₈₋₅₀. Predicted and observed masses of bypass products are indicated. The neutral mass spectrum is shown on the right. Mass is shown on the x axis, decreasing from left to right, and abundance is shown on the y axis. (B) Disruption of base pairing in the lower part of the stem-loop in construct LS-2. Mutant nucleotides are shown in light grey. Other features are the same as for (A) (C) Strengthened potential base pairing in the lower part of the stem-loop. Mutant nucleotides are shown in light grey. Other features are the same as for (A).

protein database search (Supplementary Figure S8). The overall coverage of the predicted NusA fusion protein was 88% (Supplementary Figure S9). Tryptic and chymotryptic peptides were also identified that showed forward bypassing to GCC₃₋₅, UCA₃₆₋₃₈ and UCU₅₈₋₆₀ (Supplementary Figure S7).

A second test of the potential for re-pairing to mRNA 5' of the take-off site involved a derivative construct with a single nucleotide change between the upstream landing site and the take-off site such that the chymotryptic trans-frame encoded peptide would have two amino acid substitutions (Supplementary Figure S11). This unique peptide was observed (Supplementary Figure S12) and MS/MS analysis of the oxidized, doubly charged ion confirmed the amino acid sequence (Supplementary Figure S13).

Discussion

Peptidyl-tRNA does not scan the coding gap

The results indicate that the anticodon of the peptidyl-tRNA resident in the ribosomal P-site during gene 60 programmed bypassing does not scan the first 47 nt of the WT coding gap mRNA as it threads through the ribosome, but does recognize and pair with the matched triplet at positions 48–50. Evidence for the lack of peptidyl-tRNA scanning until the end of the WT coding gap comes from the observations of (1) landing only at GGA₄₈₋₅₀ with a WT gene 60 cassette, although there is a potential landing site at GGG₉₋₁₁, (2) landing only at an introduced AUU₄₈₋₅₀ from an AUU take-off site, although there are three naturally occurring AUU triplets within the coding gap, (3) peptidyl-tRNA^{Lys} landing

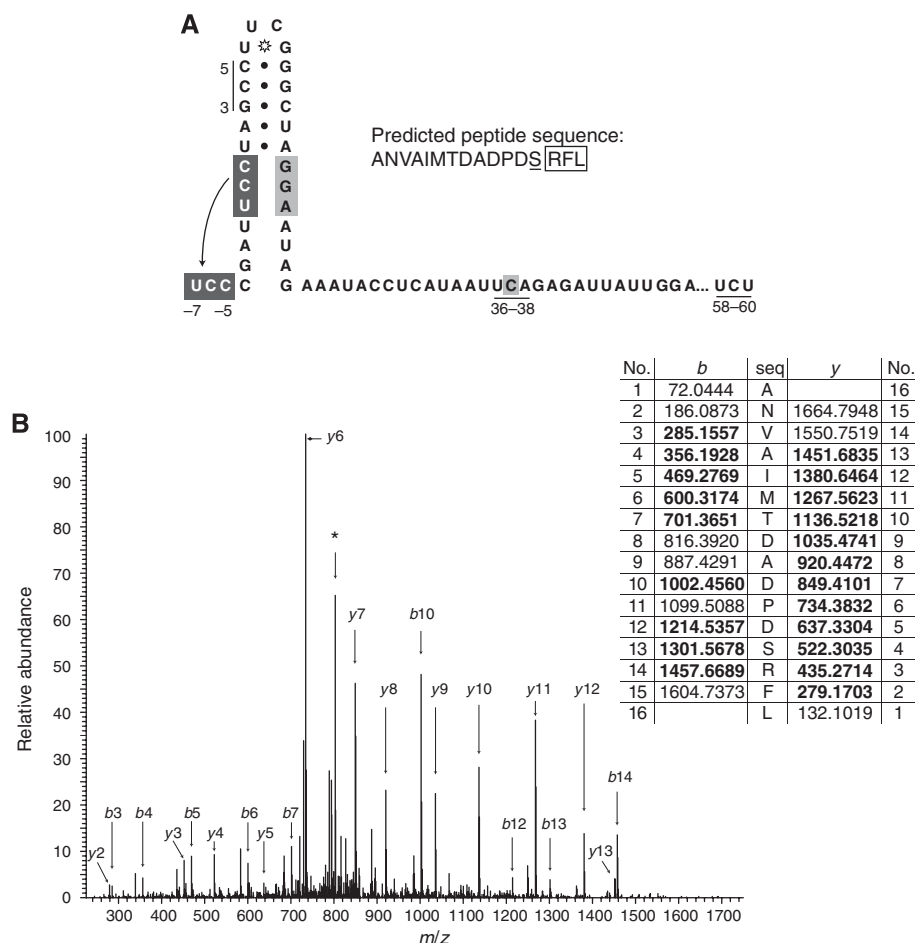


Figure 8 Backwards bypassing. (A) Sequence and potential secondary structure of a construct designed to detect backwards bypassing. The take-off codon, UCC, and a matched codon 7–5 nt 5' are shown in white letters in dark grey boxes. Compensatory changes made to maintain base-pairing potential in the 5' stem-loop are shown in light grey. A₃₇ was changed to C, light grey, to eliminate a stop codon in the same frame as UCC_{-7 to -5}. The amino acid sequence of a predicted chymotryptic peptide of the backwards bypass product is shown where S, encoded by the take-off codon, is underlined and the amino acids encoded after landing at UCC_{-7 to -5} are boxed. Alternative landing sites are underlined. (B) MS/MS data of the trans-frame chymotryptic peptide. The x axis is mass to charge ratio, *m/z*, and the y axis is relative abundance. Many 'b' series ions and 'y' series ions supporting the sequence were identified in the spectrum (arrows). * indicates a prominent ion corresponding to the doubly charged b15 species. Predicted masses of peptides are shown in the right-hand table; those shown in bold were identified.

only within a run of six introduced A residues beginning at position 48, although there are two other potential productive landing sites, AAA₂₂₋₂₄ and AAG₃₇₋₃₉ and (4) landing only at an introduced GAG₄₈₋₅₀ from a GAG take-off site, although there is a GAG triplet 6 nt 5' at positions 39–41.

Internal SD effects on bypassing ribosomes

The SD-like sequence, GAG₃₉₋₄₁, influences the efficiency of bypassing as determined by mutagenesis and by the use of specialized ribosomes (SD:anti-SD swapping experiments). It functions by contributing to the initiation of scanning by the anticodon of peptidyl-tRNA. This effect is most clearly demonstrated in the construct containing a GAG take-off site and three introduced GAG sequences spaced 6 nt apart in the coding gap, where landing occurs predominantly at the second GAG₃₀₋₃₂ sequence (i.e. the first available landing site 3' of a potential SD-like GAG₂₁₋₂₃). However, the SD effect cannot account entirely for the initiation of peptidyl-tRNA scanning as a substantial amount of landing occurs at the same position, GAG₃₀₋₃₂, in a related construct lacking the first introduced GAG₂₁₋₂₃ sequence. Further, the SD influence on landing of the WT GAG₃₉₋₄₁ is modest, as, for bypassing

ribosomes with UCC-decoding peptidyl-tRNA, substitution of the WT SD-like GAG₃₉₋₄₁ with CAC causes predominant landing at the WT-positioned UCC₄₈₋₅₀ and only a minor amount of landing at the 3' adjacent UCC₅₁₋₅₃. (In non-programmed bypassing, landing can occur at multiple sites—the first potential site does not 'trap' all the scanning ribosomes (Herr *et al*, 2004).)

The 5' stem-loop

Although the nature of mRNA structure(s) of the 50 nt coding gap is unknown, sequence in the 5' part of the coding gap is involved in a stem-loop structure important for bypassing. Disruption of the upper portion of the 5' stem-loop, by affecting base pairing in the stem or altering the tetraloop, can allow peptidyl-tRNA^{Gly} to pair with GGG₉₋₁₁ that is normally hidden in the WT structure. The existence of the lower part of the stem-loop is supported by mutagenesis studies where the stability of the predicted base pairing was decreased or increased, and by the demonstrations of backwards bypassing. Furthermore, the observation of landing at an introduced GAG site that lacks a 5' SD sequence and the effects of some mutants of the distal two-thirds of the coding

gap are consistent with structure of the entire coding gap (manuscript in preparation).

The 5' stem-loop could be sensed by the leading edge of the ribosome, or at the mRNA unwinding site before decoding of the take-off codon, GGA. If so, the ribosome would need to retain some 'memory' of the stimulation until the GGA enters the P-site. In addition, certain of the mutants with base substitutions would have to impart an 'altered memory' so that landing could occur within the gap. This scenario seems unlikely and is undermined by the demonstration of backwards bypassing that supports formation of the 5' stem-loop structure after take-off. We conclude, in agreement with the suggestion of Herbst *et al* (1994), that the GGA take-off codon is involved in base pairing after it has been decoded. (This proposal emanated from a study using a debilitated bypassing cassette with 15 extra base pairs inserted at the top of the 5' stem-loop and identification of a compensatory mutant of ribosomal protein L9. Further work showed that the role of ribosomal protein L9 is to restrain forward mRNA slippage (Herr *et al*, 2001a).)

Where does the stem-loop containing structure reside within the ribosome? Previous work has shown that RF1, within its normal concentration range, is precluded from the A-site at take-off during bypassing (Herr *et al*, 2000b). We propose that mRNA structure most likely occupies the A-site, but it may extend into the inter-subunit space. This situation is comparable to one in which tRNA was artificially excluded from the A-site that showed the propensity of mRNA to occupy the A-site and form structure (Yusupova *et al*, 2001). It has been suggested that when a tmRNA-SmpB complex enters the A-site of a stalled ribosome, the linker helix of tmRNA mimics the long variable arm of class II tRNAs and occupies the inter-subunit space (Bessho *et al*, 2007).

Perhaps a formal parallel to the proposed entry of coding gap mRNA into the ribosome is the 'scrunching' of downstream DNA into RNA polymerase. Although this has been shown to occur as a prelude to the escape of RNA polymerase from promoter contacts (Kapanidis *et al*, 2006; Revyakin *et al*, 2006), the potential parallel is greater to predicted DNA 'scrunching' into transcription complexes paused during elongation (Roberts, 2006).

A model for bypassing

We propose a model invoking mRNA structure formation within the ribosome being central to bypassing (Figure 9). In this model, the take-off stem-loop exerts its effect on bypassing after decoding of GGA. After codon 46, GGA, is decoded, and the occurrence of standard ribosome unlocking, the GGA enters the ribosomal P-site, whereas the 3' adjacent UAG moves into the A-site. The model envisages several likely interconnected events then occurring. The UAG stop codon in the A-site is slow to decode. The pause facilitates 3' nt entering the A-site, perhaps aided by distortion caused by the nascent peptide signal (Figure 9A). The tendency of this mRNA to immediately form a hairpin structure capped by a tetraloop aids initiation of formation of the 5' stem-loop requiring 'pulling' mRNA initially from the 3' direction into the A-site. While this is occurring, or closely following it, the P-site codon, GGA, and the anticodon of peptidyl-tRNA dissociate, facilitated by the effect(s) of the nascent 'special' peptide sequence 15–30 amino acids from the peptidyl

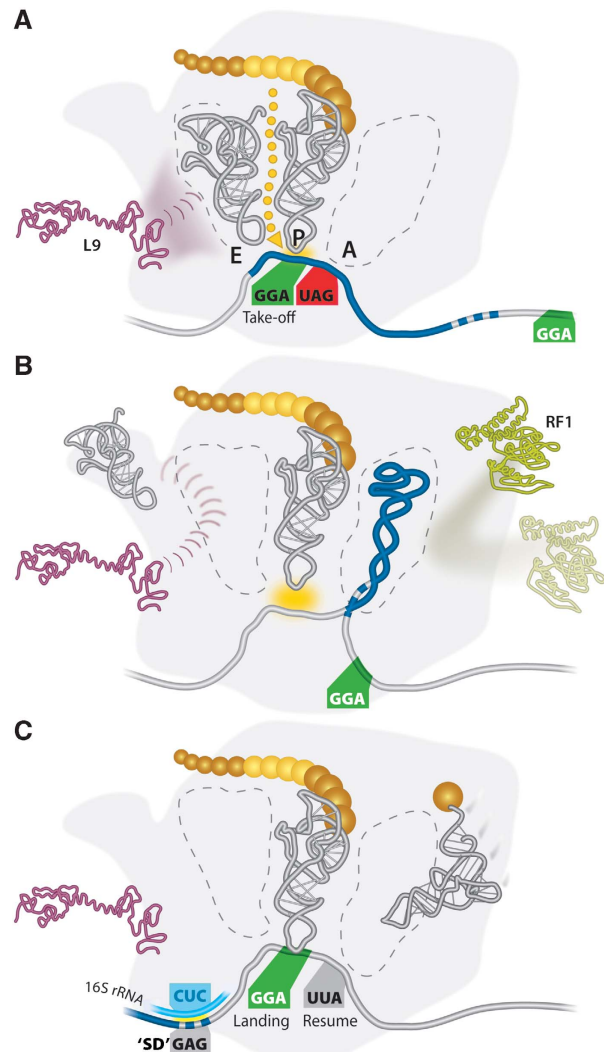


Figure 9 Model for programmed bypassing. (A) The A-, P- and E-sites of the ribosome are filled with RNA or shown by a dotted outline. The indirect influence of the segment of the nascent peptide (yellow) on peptidyl-tRNA anticodon: GGA 'take-off' codon (green flag) dissociation is indicated by a dotted line. The UAG (red flag) in the A-site causes a pause that permits extra mRNA (dark blue) to start to enter the A-site, where it forms a structure diagrammed in (B). The SD-like GAG sequence in the coding gap (dark blue dashes in the mRNA) and the landing site codon, GGA (white letters on green flag) are indicated. (B) Intra-mRNA pairing drags mRNA initially from both the 5' and 3' directions to allow formation of the 5' stem-loop. Occupancy of the A-site by structure precludes entry by release factor 1 (pale green) and permits E-site tRNA exit mediated by L9 (purple). Forward RNA movement 'resolves' the structure in the A-site without peptidyl-tRNA scanning. (C) Return to linear mRNA and pairing of GAG (grey flag) 6 nt 5' of the end of the coding gap to the 3' end of 16S rRNA (light blue) contributes to the initiation of peptidyl-tRNA scanning and pairing to the landing site, GGA (green flag). Standard decoding resumes at the adjacent 3' codon, UUA (grey flag).

transfer site and by continuing stem formation as it now 'pulls' mRNA from the 5' and 3' directions. Structure formation and base pairing of the stop codon within the stem-loop precludes RF1 access (Figure 9B). The remaining coding gap mRNA, including the SD-like GAG and the two following AUU triplets, then enters the A-site. Coding gap mRNA structure (Figure 9B) forms in space normally occupied by RF or tRNA

(although some of the structure may be in the inter-subunit space). Occupancy of the A-site tRNA position by mRNA is indirectly sensed (through ratcheting?) by ribosomal protein L9 (Figure 9B) and it, in turn, influences the L1 stalk/protuberance movement (Schuwirth *et al*, 2005). This directly, or more likely indirectly (see below) helps liberate mRNA for forward mRNA slippage.

As the coding gap mRNA exits the A-site and passes through the P-site, it is not scanned by the peptidyl-tRNA anticodon, possibly because the normal mRNA kink between the A- and P-sites is affected by A-site mRNA structure. After this mRNA leaves the E-site, it is scanned by the anti-SD sequence near the 3' end of 16S rRNA. Formation of a weak rRNA anti-SD interaction with a complementary sequence in mRNA (Figure 9C) indirectly contributes to the anticodon of peptidyl-tRNA scanning of the transiting mRNA where in WT, the GGA₄₈₋₅₀ would be in the normal mRNA position in the P-site. (Other work has shown that an SD:anti-SD interaction influences the path of intra-ribosomal mRNA (Yusupova *et al*, 2006; Jenner *et al*, 2007).) Dissipation of the intra-ribosomal mRNA structure more strongly facilitates peptidyl-tRNA scanning (and certain disruptions of the structure by base substitutions have a similar effect; see below). Continuing effects of the nascent peptide help ensure stringency, and so fidelity, of anticodon re-pairing to mRNA. As the peptidyl-tRNA anticodon pairs with the landing site codon, GGA, the resume codon, UUA (codon 47) is present as linear mRNA in the A-site (Figure 9C). Cognate tRNA is now free to enter the vacant tRNA space in the A-site allowing resumption of standard peptidyl-transfer and translation.

An indirect effect of L9 could be through allowing E-site tRNA departure. Nierhaus has proposed that the ribosome senses A-site occupancy before permitting E-site tRNA exit to ensure that the anticodons of two tRNAs are paired to mRNA to reduce mRNA slippage potential (for review, see Wilson and Nierhaus, 2006). Although some of the many *in vitro* tests of aspects of the allosteric model have yielded controversial results, the mRNA in the E-site is positioned with the potential for anticodon pairing (Jenner *et al*, 2007), and *in vivo* experiments on frameshifting (Baranov *et al*, 2002; Sanders and Curran, 2007) are supportive of E-site tRNA anticodon:codon pairing. As the gene 60 model involves A-site mRNA structure rather than tRNA, it potentially provides a distinction between ribosome movements involving A-site tRNA space occupancy and those due to delivery of the aminoacyl-tRNA EF-Tu ternary complex.

The issue of what drives the forward movement of mRNA during bypassing and the associated internal unwinding of mRNA structure requires further investigation.

The model provides a rationale for the absence of peptidyl-tRNA anticodon scanning of the WT coding gap, how certain mutants of the gap cause peptidyl-tRNA scanning to commence at internal positions and how backwards bypassing can occur.

Comparison with mRNA structures occupying ribosomal P- and A-sites

In gene 60 bypassing, there is a peptidyl-tRNA in the ribosomal P-site. In contrast, in dicistrovirus intergenic initiation, one of the mRNA IRES pseudoknots occupies the P-site (Schüler *et al*, 2006) where it apparently exerts an effect as a codon:anticodon stem-loop mimic. There it functionally

replaces tRNA Met-i permitting remarkable methionine-independent initiation, which occurs in the A-site (Jan *et al*, 2003; Hatakeyama *et al*, 2004). In gene 60 bypassing, the coding gap mRNA structure postulated to occupy (at least partially) the A-site has the same effect as tRNA on ribosomal protein L9's gating effect on E-site tRNA exit.

Translation initiation and coding resumption in gene 60 translation occur on the same mRNA, whereas coding resumption occurs on a separate mRNA when tmRNA exerts an effect in the A-site to rescue stalled ribosomes (which could also be termed *trans*-bypassing as the resume codon is at an internal position in tmRNA). Similar to gene 60, structural features of tmRNA are important.

Broader implications of intra-ribosomal mRNA structure

Slow A-site decoding increases the possibility of formation of an mRNA stem-loop, and together with a high potential for codon:anticodon dissociation, is important for the initiation of bypassing. Intra-ribosomal mRNA structure formation is, itself, likely to contribute to the extent of a pause. Perhaps this hypothetical extended pausing is important in some cases even without the involvement of bypassing and could involve less stable stem-loop structures. In addition, where bypassing is not utilized, the potential for mRNA structure involving sequences flanking stop codons may be under negative selection.

Materials and methods

Bacterial strains

E. coli K-12 SU1675 {*ara* Δ(*pro-lac*), *recA56*, *thi* F' [*proAB*⁺ *lacI*^F]} was used as a host strain in all of the specialized ribosome experiments and for all DNA manipulations (Miller, 1972). *E. coli* BL21(DE3) F⁻ *opm*⁺ *hdsSB* (rB⁻ mB⁻) *gal dcm* (DE3) lambda lysogen was used as a host strain for all the protein expression experiments.

Construction of pNTH vector and derivatives

The parent vector for the construction of the NusA-gene 60 fusions was pET43.1 (Novagen). A 5' 6 histidine tag was removed by deleting the sequence between the *SpeI* and *SacII* sites. A small linker sequence, CTAGACGTACGTACGC, was then cloned between these sites to maintain the reading frame. Next the TRI-HIS encoding sequence, CATCATCATCATCATATTAGGCACCACCAC CACCACCCTAG GCATCATCATCATCATCAT, was cloned between the *PstI* and *KpnI* sites to produce pNTH-2. Finally, mutant gene 60 sequences produced by two-step PCR using primers with embedded restriction sites were cloned 3' and in-frame with the NusA and S-tag sequences, between the *SpeI* and *EcoRI* sites. A modification of the WT gene 60 construct was made to test for landing within the coding gap (see Figure 3) by adding a 6 × histidine tag 5' of the gene 60 sequence and by introducing stop codons in all three frames 3' of the WT landing site.

β-Galactosidase activity assays

β-Galactosidase activity assays were performed using the whole-cell assay procedure of Miller (1972). All assays were performed in triplicate on several independent clones. A more detailed description of the specialized ribosome experiments is included in Supplementary data.

Protein purification and pulse-chase analysis

Cultures were grown as previously described (Herr *et al*, 2004). Harvested cells were lysed using BugBuster (Novagen), and NusA-S-tag-gene 60-6 × HIS protein(s) was purified by sequential chromatography on Ni-NTA agarose (Qiagen) and S-protein agarose (Novagen). Eluted protein was concentrated and washed twice with dH₂O using Centricon 50 (Millipore) filtration devices. Pulse-chase analysis was performed as previously described (Herr *et al*, 1999).

Mass spectrometry

ESI/MS (Herr et al, 2004) and LC/MS/MS (Atkins et al, 2007) were performed as previously described. More detailed descriptions are available in Supplementary data.

Supplementary data

Supplementary data are available at *The EMBO Journal* Online (<http://www.embojournal.org>).

References

Atkins JF, Wills NM, Loughran G, Wu CY, Parsawar K, Ryan MD, Wang CH, Nelson CC (2007) A case for 'StopGo': reprogramming translation to augment codon meaning of GGN by promoting unconventional termination (Stop) after addition of glycine and then allowing continued translation (Go). *RNA* **6**: 803–810

Babinger K, Hallmann A, Schmitt R (2006) Translational control of regA, a key gene controlling cell differentiation in *Volvox carterii*. *Development* **133**: 4045–4051

Baranov PV, Gesteland RF, Atkins JF (2002) Release factor 2 frameshifting sites in different bacteria. *EMBO Rep* **3**: 373–377

Bessho Y, Shibata R, Sekine S I, Murayama K, Higashijima K, Hori-Takemoto C, Shirouzu M, Kuramitsu S, Yokoyama S (2007) Structural basis for functional mimicry of long-variable-arm tRNA by transfer-messenger RNA. *Proc Natl Acad Sci USA* **104**: 8293–8298

Bucklin DJ, Wills NM, Gesteland RF, Atkins JF (2005) P-site pairing subtleties revealed by the effects of different tRNAs on programmed translational bypassing where anticodon re-pairing to mRNA is separated from dissociation. *J Mol Biol* **345**: 39–49

Chappell SA, Dresios J, Edelman GM, Mauro VP (2006) Ribosomal shunting mediated by a translational enhancer element that base pairs to 18S rRNA. *Proc Natl Acad Sci USA* **103**: 9488–9493

Chen H, Bjerknes M, Kumar R, Jay E (1994) Determination of the optimal aligned spacing between the Shine–Dalgarno sequence and the translation initiation codon of *Escherichia coli* mRNAs. *Nucleic Acids Res* **22**: 4953–4957

Chittum HS, Lane WS, Carlson BA, Roller PP, Lung FD, Lee BJ, Hatfield DL (1998) Rabbit β -globin is extended beyond its UGA stop codon by multiple suppressions and translational reading gaps. *Biochemistry* **37**: 10866–10870

Gallant J, Bonthuis P, Lindsley D (2003) Evidence that the bypassing ribosome travels through the coding gap. *Proc Natl Acad Sci USA* **100**: 13430–13435

Gallant JA, Lindsley D (1998) Ribosomes can slide over and beyond 'hungry' codons, resuming protein chain elongation many nucleotides downstream. *Proc Natl Acad Sci USA* **95**: 13771–13776

Hatakeyama Y, Shibuya N, Nishiyama T, Nakashima N (2004) Structural variant of the intergenic internal ribosome entry site elements in dicistroviruses and computational search for their counterparts. *RNA* **10**: 779–786

Hemmings-Mieszczyk M, Hohn T, Preiss T (2000) Termination and peptide release at the upstream open reading frame are required for downstream translation on synthetic shunt-competent mRNA leaders. *Mol Cell Biol* **20**: 6212–6223

Herbst KL, Nichols LM, Gesteland RF, Weiss RB (1994) A mutation in ribosomal protein L9 affects ribosomal hopping during translation of gene 60 from bacteriophage T4. *Proc Natl Acad Sci USA* **91**: 12525–12529

Herr AJ, Atkins JF, Gesteland RF (1999) Mutations which alter the elbow region of tRNAGly2 reduce T4 gene 60 translational bypassing efficiency. *EMBO J* **18**: 2886–2896

Herr AJ, Atkins JF, Gesteland RF (2000a) Coupling of open reading frames by translational bypassing. *Annu Rev Biochem* **69**: 343–372

Herr AJ, Gesteland RF, Atkins JF (2000b) One protein from two open reading frames: mechanism of a 50 nt translational bypass. *EMBO J* **19**: 2671–2680

Herr AJ, Nelson CC, Wills NM, Gesteland RF, Atkins JF (2001a) Analysis of the roles of tRNA structure, ribosomal protein L9, and the bacteriophage T4 gene 60 bypassing signals during ribosome slippage on mRNA. *J Mol Biol* **309**: 1029–1048

Herr AJ, Wills NM, Nelson CC, Gesteland RF, Atkins JF (2001b) Drop-off during ribosome hopping. *J Mol Biol* **311**: 445–452

Acknowledgements

We thank Dr K Parsawar for help with peptide LC/MS/MS analysis, Tara Atkins for expert technical help, Sheila Avery and Susan Roberts for help with figures and Dr D Shub for sharing unpublished data. This study was supported by NIH RO1 grant GM079523 and a personal award from Science Foundation Ireland to JFA.

Herr AJ, Wills NM, Nelson CC, Gesteland RF, Atkins JF (2004) Factors that influence selection of coding resumption sites in translational bypassing: minimal conventional peptidyl-tRNA pairing can suffice. *J Biol Chem* **279**: 11081–11087

Huang WM, Ao SZ, Casjens S, Orlandi R, Zeikus R, Weiss R, Winge D, Fang M (1988) A persistent untranslated sequence within bacteriophage T4 DNA topoisomerase gene 60. *Science* **239**: 1005–1012

Jan E, Kinzy TG, Sarnow P (2003) Divergent tRNA-like element supports initiation, elongation, and termination of protein biosynthesis. *Proc Natl Acad Sci USA* **100**: 15410–15415

Jenner L, Rees B, Yusupov M, Yusupova G (2007) Messenger RNA conformations in the ribosomal E site revealed by X-ray crystallography. *EMBO Rep* **8**: 846–850

Jin H, Zhao Q, de Valdivia EIG, Ardell DH, Stenström M, Isaksson LA (2006) Influences on gene expression *in vivo* by a Shine–Dalgarno sequence. *Mol Microbiol* **60**: 480–492

Kane JF, Violand BN, Curran DF, Staten NR, Duffin KL, Bogosian G (1992) Novel in-frame two codon translational hop during synthesis of bovine placental lactogen in a recombinant strain of *Escherichia coli*. *Nucleic Acids Res* **20**: 6707–6712

Kapanidis AN, Margeat E, Ho SO, Kortkhonjia E, Weiss S, Ebright RH (2006) Initial transcription by RNA polymerase proceeds through a DNA-scrunching mechanism. *Science* **314**: 1144–1147

Klovins J, Tsareva NA, de Smit MH, Berzins V, van Duin J (1997) Rapid evolution of translational control mechanisms in RNA genomes. *J Mol Biol* **265**: 372–384

Larsen B, Wills NM, Gesteland RF, Atkins JF (1994) rRNA–mRNA base pairing stimulates a programmed –1 ribosomal frameshift. *J Bacteriol* **176**: 6842–6851

Larsen B, Wills NM, Nelson CC, Atkins JF, Gesteland RF (2000) Nonlinearity in genetic decoding: homologous DNA replicase genes use alternatives of transcriptional slippage or ribosomal frameshifting. *Proc Natl Acad Sci USA* **97**: 1683–1688

Miller ES, Kutter E, Mosig G, Arisaka F, Kunisawa T, Rüger W (2003) Bacteriophage T4 genome. *Microbiol Mol Biol Rev* **67**: 86–156

Miller JH (1972) *Experiments in Molecular Genetics*. Cold Spring Harbor, New York, USA: Cold Spring Harbor Laboratory Press

Murgola EJ, Pagel FT (1980) Codon recognition by glycine transfer RNAs of *Escherichia coli in vivo*. *J Mol Biol* **138**: 833–844

O'Connor M, Gesteland RF, Atkins JF (1989) tRNA hopping: enhancement by an expanded anticodon. *EMBO J* **8**: 4315–4323

Revyakin A, Liu C, Ebright RH, Strick TR (2006) Abortive initiation and productive initiation by RNA polymerase involve DNA scrunching. *Science* **314**: 1139–1143

Roberts JW (2006) RNA polymerase, a scrunching machine. *Science* **314**: 1097–1098

Sanders CL, Curran JF (2007) Genetic analysis of the E site during RF2 programmed frameshifting. *RNA* **13**: 1483–1491

Schüler M, Connell SR, Lescoute A, Giesebrecht J, Dabrowski M, Schroer B, Mielke T, Penczek PA, Westhof E, Spahn CMT (2006) Structure of the ribosome-bound cricket paralysis virus IRES RNA. *Nat Struct Mol Biol* **13**: 1092–1096

Schuwirth BS, Borovinskaya MA, Hau CW, Zhang W, Vila-Sanjurjo A, Holton JM, Cate JHD (2005) Structures of the bacterial ribosome at 3.5 Å resolution. *Science* **310**: 827–834

Unoson C, Wagner EGH (2007) Dealing with stable structures at ribosomal binding sites. *RNA Biol* **4**: 113–117

Weiss RB, Dunn DM, Atkins JF, Gesteland RF (1987) Slippery runs, shifty stops, backward steps, and forward hops: –2, –1, +1, +2,

- +5, and +6 ribosomal frameshifting. *Cold Spring Harb Symp Quant Biol* **52**: 687–693
- Weiss RB, Huang WM, Dunn DM (1990) A nascent peptide is required for ribosomal bypass of the coding gap in bacteriophage T4 gene 60. *Cell* **62**: 117–126
- Wills NM, Ingram JA, Gesteland RF, Atkins JF (1997) Reported translational bypass in a *trpR'*-*lacZ'* fusion is accounted for by unusual initiation and +1 frameshifting. *J Mol Biol* **271**: 491–498
- Wilson DN, Nierhaus KH (2006) The E-site story: the importance of maintaining two tRNAs on the ribosome during protein synthesis. *Cell Mol Life Sci* **63**: 2725–2737
- Xi Q, Cuesta R, Schneider RJ (2005) Regulation of translation by ribosome shunting through phosphotyrosine-dependent coupling of adenovirus protein 100k to viral mRNAs. *J Virol* **79**: 5676–5683
- Yueh A, Schneider RJ (2000) Translation by ribosome shunting on adenovirus and Hsp70 mRNAs facilitated by complementarity to 18S rRNA. *Gene Develop* **14**: 414–421
- Yusupova G, Jenner L, Rees B, Moras D, Yusupov M (2006) Structural basis for messenger RNA movement on the ribosome. *Nature* **444**: 391–394
- Yusupova GZ, Yusupov MM, Cate JHD, Noller HF (2001) The path of messenger RNA through the ribosome. *Cell* **106**: 233–241